Derivatives of $[Rh_6(CO)_{13}C]^{2-}$: Solution Structure of $[Rh_6H(CO)_{13}C]^-$ from Nuclear Magnetic Resonance Measurements and the *X*-Ray Crystal Structure of $[Rh_6(CO)_{11}C(\mu\text{-}Ph_2PCH_2CH_2PPh_2)]^{2-}$ †

Silvia Bordoni, Brian T. Heaton,* Claudio Seregni, and Luisella Strona
Department of Inorganic, Physical and Inorganic Chemistry, University of Liverpool, Liverpool L69 3BX
Robin J. Goodfellow
Department of Inorganic Chemistry, The University of Bristol, Bristol BS8 1TS
Michael B. Hursthouse and Mark Thornton-Pett
Department of Chemistry, Queen Mary College, London E1 4NS
Secondo Martinengo
Centro Sintesi e Struttura dei Composti dei Metalli di Transizione nei Bassi Stati di Ossidazione, Via G. Venezian 21, 20133 Milano, Italy

---

Multielement n.m.r. measurements (^1H, ^1H-{^{103}Rh}, ^{13}C, ^{13}C-{^{103}Rh}, and ^{103}Rh) show that protonation of $[Rh_6(CO)_{13}C]^{2-}$ at low temperature gives $[Rh_6H(CO)_{13}C]^-$ which contains an edge-bridging hydride with the carbonyl distribution being very similar to that found in $[Rh_6(CO)_{13}C]^{2-}$ Warming this solution to < -20 °C results in complete CO- and H-migration over the Rh_6 octahedron and at $\geqslant -20$ °C there is formation of $[Rh_6H(CO)_{15}C]^-$ together with loss of hydrogen to give $[Rh_{12}(CO)_{24}(C)_2]^{2-}$ which has been spectroscopically characterised. Multielement n.m.r. studies on products resulting from the reaction of $[Rh_6(CO)_{13}C]^{2-}$ (1 mol equiv.) with diphosphines $Ph_2P(CH_2)_nPPh_2$ [0.5 mol equiv.; n = 1, 2 (dppe), 3, or 4] or $Ph_2AsCH_2CH_2AsPh_2$ suggest that they all have similar structures and an *X*-ray crystallographic analysis of the dppe derivative shows it to be $[Rh_6(CO)_{11}C(\mu\text{-dppe})]^{2-}$.

Cobalt and rhodium can form both octahedral and trigonal prismatic clusters containing either carbon or nitrogen as interstitial atoms[1-6] and these can be readily interconverted, equation (1) (M = Co or Rh; E = C, n = 2; E = N, n = 1).

$$\underset{M_6\text{ octahedron}}{[M_6(CO)_{13}E]^{n-}} \underset{-2CO}{\overset{+2CO}{\rightleftharpoons}} \underset{M_6\text{ trigonal prism}}{[M_6(CO)_{15}E]^{n-}} \qquad (1)$$

Previous n.m.r. measurements[7] showed that protonation of $[Rh_6(CO)_{15}C]^{2}$ at low temperature produced $[Rh_6H(CO)_{15}C]^-$ with the hydride occupying a triangular face of the trigonal prismatic skeleton whereas the related cluster, $[Rh_6H(CO)_{15}]^-$, contained a terminal hydride and adopted a structure analogous to the octahedral clusters, $[Rh_6(CO)_{15}X]^-$ (X = I,[8] COEt,[9] or CO_2Me[9]). Both these hydride derivatives lost hydrogen on warming to give dimeric products, $[Rh_{12}(CO)_{24}(C)_2]^{2-}$ and $[Rh_{12}(CO)_{30}]^{2-}$ respectively.[7] It was therefore of interest to investigate the analogous protonation reaction of the octahedral cluster, $[Rh_6(CO)_{13}C]^{2-}$; this gives $[Rh_6H(CO)_{13}C]^-$ which we now show, using multielement n.m.r., adopts a structure very similar to the precursor with the hydride occupying an edge-bridging position at low temperature. At higher temperatures ($\leqslant -20$ °C), complete carbonyl *and* H-migration occurs around the Rh_6 octahedron; this presently provides a unique example of H and CO *both* migrating over the same skeleton.

Although numerous substituted neutral metal carbonyl clusters are now known, the ligand site preference is still poorly understood and the reaction of anionic carbonyl clusters with phosphines or phosphites almost always leads to fragmentation. However, since interstitial atoms tend to stabilise metal polyhedra and because of the ease of reaction of $[Rh_6(CO)_{13}C]^{2-}$ with CO [equation (1)], it was of interest to investigate the reaction of $[Rh_6(CO)_{13}C]^{2-}$ with chelating diphosphines (L–L) and chelating diarsines ($Ph_2AsCH_2CH_2AsPh_2$, dpae). We now report n.m.r. measurements on products resulting from the reaction of $[Rh_6(CO)_{13}C]^{2-}$ with either L–L ($Ph_2PCH_2PPh_2$, dppm; $Ph_2PCH_2CH_2PPh_2$, dppe; $Ph_2PCH_2CH_2CH_2PPh_2$, dppp; $Ph_2PCH_2CH_2CH_2CH_2PPh_2$, dppb) or dpae. They suggest that similar products are formed and an *X*-ray crystal structure on the dppe derivative shows it to be $[Rh_6(CO)_{11}C(\mu\text{-dppe})]^{2-}$ with the dppe ligand occupying the same edge as the bridging hydride in $[Rh_6H(CO)_{13}C]^-$.

Results and Discussion

$[Rh_6H(CO)_{13}C]^-$.—Addition of excess acid (CF_3CO_2H) to a solution of $[Rh_6(CO)_{13}C]^{2-}$ in CD_2Cl_2 at −76 °C produces $[Rh_6H(CO)_{13}C]^-$ which is shown by multielement n.m.r. measurements at low temperature to adopt the structure shown in Figure 1(*a*).

At −85 °C the 100-MHz ^1H n.m.r. spectrum consists of a triplet [$\delta(^1H)$ −14.6 p.p.m., $^1J(^{103}Rh_A\text{-}^1H)$ 20 Hz] and ^1H-{^{103}Rh} INDOR measurements show coupling to only one type of rhodium, $\delta(^{103}Rh_A)$ −749 p.p.m. Non-^1H-decoupled direct ^{103}Rh n.m.r. measurements at −90 °C show there to be three equally intense resonances at −288, −749, and −996 p.p.m. with only the resonance at −749 p.p.m. appearing as a doublet due to H-coupling. This is consistent with the C_2 symmetry of the structure shown in Figure 1(*a*) and in agreement with this are the 90.6-MHz ^{13}C n.m.r. spectra (Figure 2) and 25-MHz ^{13}C-{^{103}Rh} n.m.r. spectra obtained at −100 °C. There are three equally intense doublets at 192.2, 193.6, and 195.2 p.p.m. due to the three pairs of terminal

---

† 5,6-μ-[1,2-Bis(diphenylphosphino)ethane]-μ_6-carbido 1,2;1,3;2,6;-3,4:1,2;1,3;2,6;3.4:4,5-penta-μ-carbonyl-1,2,3,4,5,6-hexa-carbonyl-*octa-hedro*-hexarhodate(2−).

Supplementary data available: see Instructions for Authors, *J. Chem. Soc., Dalton Trans.*, 1988, Issue 1, pp. xvii—xx.

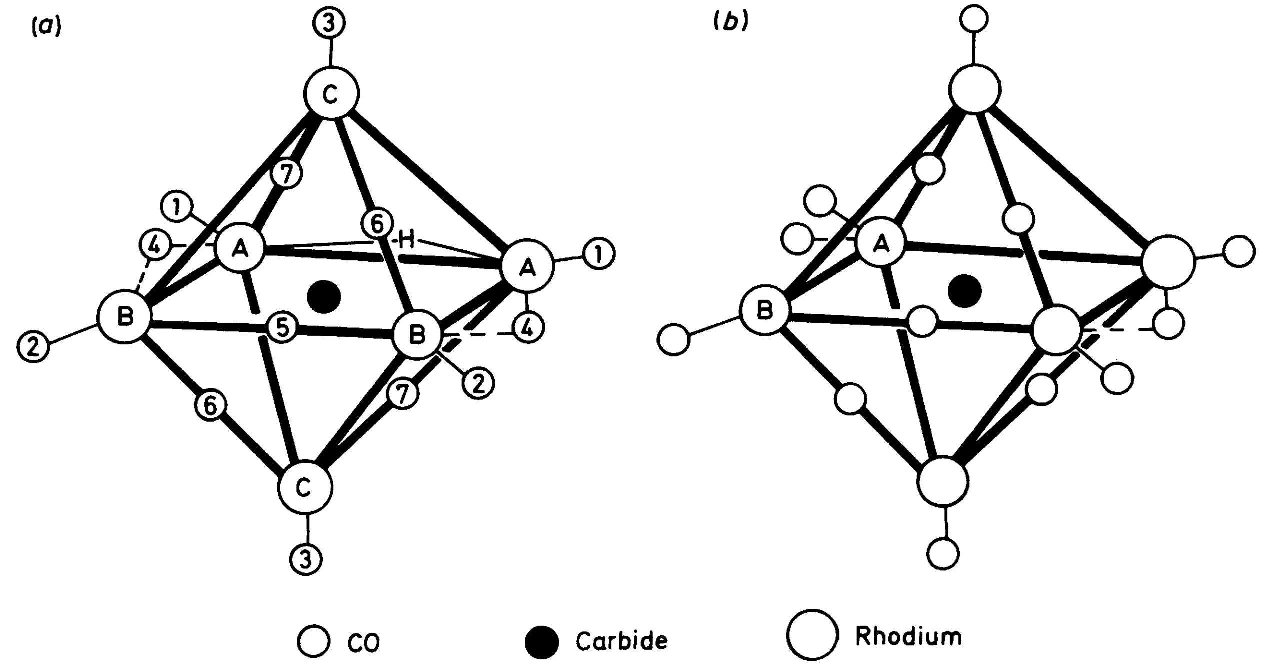

Figure 1. Schematic representation of the structures of (*a*) $[Rh_6H(CO)_{13}C]^-$ and (*b*) $[Rh_6(CO)_{13}C]^{2-}$ (ref. 1)

Table 1. N.m.r. data for $[NEt_4][Rh_6H(CO)_{13}C]$ in CD_2Cl_2 at low temperatures*

$\delta(H)$/p.p.m.	−14.6
$\delta(Rh_A)$/p.p.m.	−749
$\delta(Rh_B)$/p.p.m.	−288
$\delta(Rh_C)$/p.p.m.	−996
$\delta(CO^1)$/p.p.m.	192.2
$\delta(CO^2)$/p.p.m.	193.6
$\delta(CO^3)$/p.p.m.	195.2
$\delta(CO^4)$/p.p.m.	209.0
$\delta(CO^5)$/p.p.m.	215.5
$\delta(CO^6)$/p.p.m.	235.7
$\delta(CO^7)$/p.p.m.	231.7
$\delta(C_{carbide})$/p.p.m.	460.4
$^1J(H-Rh_A)$/Hz	20.0
$^2J(H-CO^4)$/Hz	18.5
$^2J(H-C_{carbide})$/Hz	2.9
$^1J(Rh_A-CO^1)$/Hz	78
$^1J(Rh_B-CO^2)$/Hz	89
$^1J(Rh_C-CO^3)$/Hz	93
$^1J(Rh_A-CO^4)$/Hz	54
$^1J(Rh_B-CO^4)$/Hz	18
$^1J(Rh_B-CO^5)$/Hz	40
$^1J(Rh_B-CO^6)$/Hz	39
$^1J(Rh_C-CO^6)$/Hz	39
$^1J(Rh_A-CO^7)$/Hz	29
$^1J(Rh_C-CO^7)$/Hz	43
$^1J(Rh_A-C_{carbide})$/Hz	17
$^1J(Rh_B-C_{carbide})$/Hz	17
$^1J(Rh_C-C_{carbide})$/Hz	17

* Chemical shifts for ^1H, ^{13}C, and ^{103}Rh were obtained at −85, −100, and −90 °C respectively. See Figure 1(*a*) for designation of atoms.

carbonyls (CO^1, CO^2, and CO^3 on Rh_A, Rh_B, and Rh_C respectively), a pair of asymmetric edge-bridging carbonyls at 209.0 p.p.m. (CO^4), which are clearly coupled to the hydride ligand (Figure 2) and to Rh_A and Rh_B from $^{13}C-\{^{103}Rh\}$ measurements, a unique carbonyl bridging the edge *trans* to H (CO^5) at 215.5 p.p.m. which clearly collapses to a singlet on irradiation at the Rh_B frequency, and two equally intense pseudo-triplets due to the remaining two pairs of edge-bridging carbonyls (CO^7 and CO^6) at 231.7 and 235.7 p.p.m. respectively. Assignment of these two resonances to CO^7 and CO^6 follows from $^{13}C-\{^{103}Rh\}$ measurements which show that both resonances become doublets on irradiation at the Rh_C frequency, while only the resonance at 235.7 p.p.m. becomes a doublet on irradiation at the Rh_B frequency; the other resonance becomes a doublet on irradiation at the Rh_A frequency. All these data are summarised in Table 1.

The chemical shift of the carbide atom (460.4 p.p.m.) is found at slightly higher frequency than that found for $[Rh_6(CO)_{13}C]^{2-}$ (470.0 p.p.m.)* and the change is similar to the rather small difference in chemical shift which occurs on protonation of the related trigonal prismatic clusters, $[Rh_6(CO)_{15}C]^{2-}$ (264.7 p.p.m.) *versus* $[Rh_6H(CO)_{15}C]^-$ (291.2 p.p.m.).[7]

The structure of $[Rh_6(CO)_{13}C]^{2-}$ is rather asymmetric[1] [Figure 1(*b*)], but a very slight distortion of one terminal carbonyl on Rh_A into a semi-edge-bridging position to Rh_B is sufficient to produce a structure analogous to that found for $[Rh_6H(CO)_{13}C]^-$ [Figure 1(*a*)]. Such a distortion in $[Rh_6(CO)_{13}C]^{2-}$ should be relatively facile since it has already been shown that, whereas all the carbonyls associated with Rh_C are static, the remaining carbonyls readily migrate around the equatorial $(Rh_A)_2(Rh_B)_2$ square plane in solution[10] and also undergo considerable thermal motion in the same plane in the solid state.[11] Thus, the structures of $[Rh_6(CO)_{13}C]^{2-}$ and $[Rh_6H(CO)_{13}C]^-$ are very similar. It is presently unclear why protonation occurs on the Rh_A-Rh_A edge rather than on one of the other four non-carbonyl-bridged edges but it should be noted that dppe also bridges the same edge (see below).

The ^{13}C and ^1H n.m.r. spectra of $[Rh_6H(CO)_{13}C]^-$ change dramatically with temperature and, although it is not yet

---

* $\delta(C_{carbide})$ for $[Rh_6(CO)_{13}C]^{2-}$ has been incorrectly reported previously.[10]

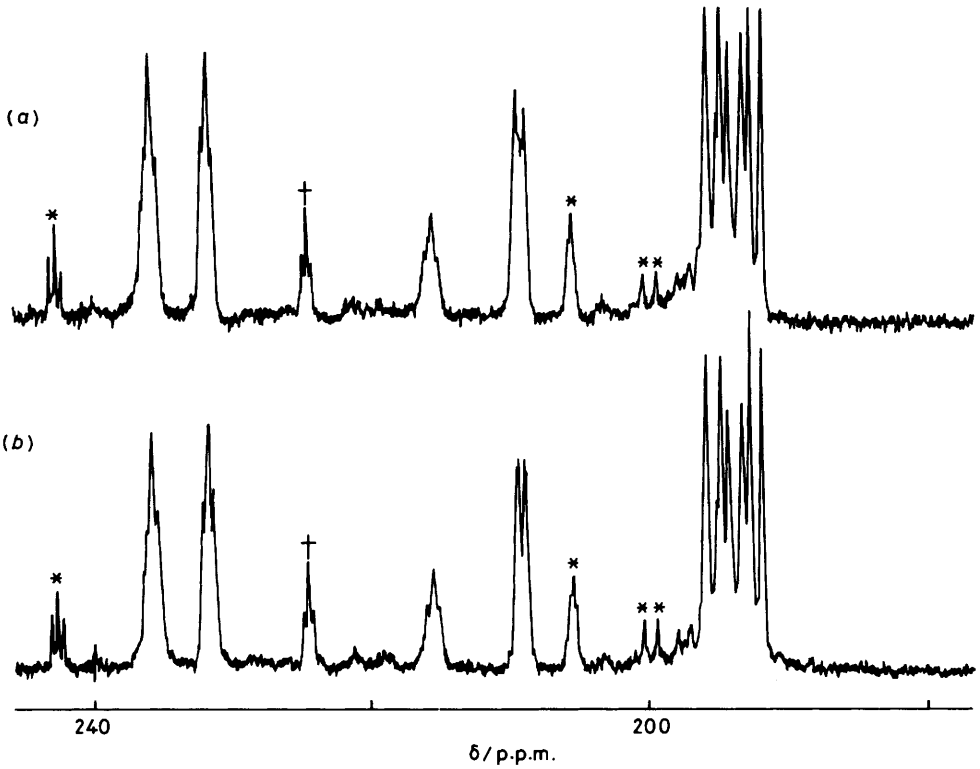

Figure 2. ^{13}C N.m.r. spectra (90.6 MHz) of $[NEt_4][Rh_6H(CO)_{13}C]$ in CD_2Cl_2 at −100 °C: (*a*) non-decoupled; (*b*) ^1H-decoupled. Impurities present: * $[Rh_6(CO)_{13}C]^{2-}$, † $[Rh_6(CO)_{15}C]^{2-}$

possible to detail the step-wise rearrangements which occur with increasing temperature, it is clear that at −20 °C there is complete randomisation of the hydride ligand over the Rh_6 skeleton. Thus, the ^1H n.m.r. spectrum is a well-resolved septet [$\delta(^1H)$ −14.6 p.p.m., $J(^{103}Rh-^1H)$ 6.6 Hz] and $^1H-\{^{103}Rh\}$ measurements show that the rhodium nuclei are all equivalent with $\delta(^{103}Rh)$ −675 p.p.m. which agrees well with the mean value of the three rhodium resonances observed at low temperature [$\delta(^{103}Rh)_{mean}$ −678 p.p.m.]. At intermediate temperatures, the direct ^{103}Rh n.m.r. clearly shows that the two resonances at highest field broaden before the resonance at −288 p.p.m. and INDOR measurements show that at −42 °C the apparent mean value of $\delta(^{103}Rh)$ is also dominated by these two resonances at −749 and −996 p.p.m., suggesting that H-migration first involves movement from the Rh_A–Rh_A edge across the $(Rh_A)_2Rh_C$ face.

The ^{13}C n.m.r. spectrum changes in a complicated way with increasing temperature and at −20 °C there is a single broad resonance at 209.7 p.p.m. [$\delta(^{13}CO)_{mean}$ 210 p.p.m.]. Unfortunately, it is impossible to carry out measurements at higher temperatures in order to reach the limiting fast-exchange carbonyl spectrum since decomposition occurs to give initially $[Rh_6H(CO)_{15}C]^-$ and then $[Rh_{12}(CO)_{24}(C)_2]^{2-}$. However, although we have previously shown there to be CO-migration around the periphery of the metallic skeleton and simultaneous interstitial H-migration in $[Rh_{13}(CO)_{24}H_{5-n}]^{n-}$ (n = 1, 2, 3, or 4) and $[Rh_{14}(CO)_{25}H]^{3-}$,[12] these measurements show for the first time in rhodium cluster chemistry that different ligands (H and CO) can both simultaneously migrate over the same metallic surface.

It is worthwhile commenting on the the n.m.r. data of $[Rh_{12}(CO)_{24}(C)_2]^{2-}$. The metal skeleton of this cluster,[13] which is related to that of $[Rh_{12}(CO)_{23}(C)_2]^{4-}$,[14] is shown schematically in Figure 3. However, it should be noted that the apparent inversion centre suggested from *X*-ray crystallographic studies is not present in solution since 12 equally intense Rh resonances [δ(Rh) 236, −33, −213, −319, −343, −531, −795, −1 003, −1 004, −1 006, −1 031, and −1 090 p.p.m.] are observed at low temperature (−80 °C), due to *all* the rhodium atoms being inequivalent. It therefore appears that either a distortion of the central Rh_4 rhomb or a distortion of one of the Rh_4 square faces occurs and either of these possibilities could be easily accommodated in the crystallographic analysis of the disorder problems associated with this structure. As expected, the ^{13}C n.m.r. spectrum at this temperature is very complicated and assignments from $^{13}C-\{^{103}Rh\}$ n.m.r. measurements have not been attempted. However, at room temperature two broad resonances at 206.7 and 200.8 p.p.m. in the ratio 2:1 respectively

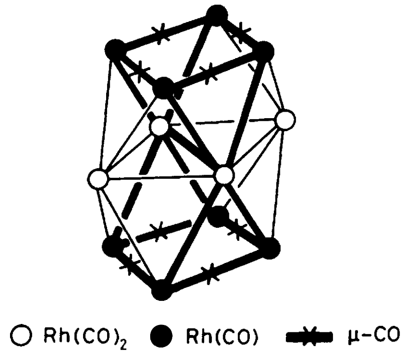

Figure 3. Schematic representation of the structure of $[Rh_{12}(CO)_{24}(C)_2]^{2-}$.[13] The interstitial carbides are each situated in the trigonal-prismatic cavities of the metallic skeleton but have been omitted for clarity

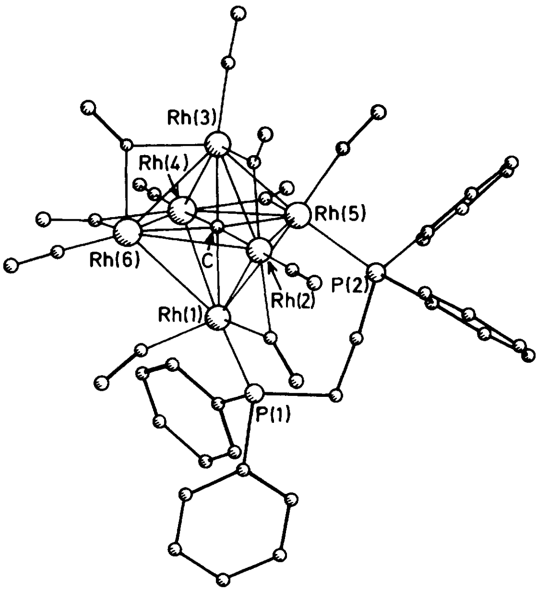

Figure 4. The $[Rh_6(CO)_{11}C(\mu\text{-dppe})]^{2-}$ anion showing the atom labelling

are observed. We attribute these to independent exchanges involving the equal number of terminal and bridging carbonyls around the separate Rh_4 square faces and to the terminal carbonyls in the Rh_4 rhomb plane exchanging *via* the unoccupied edges in this plane. Consistent with this is the fact that the resonance at lower field, 206.7 p.p.m., involves the exhange of the bridging carbonyls which are on the Rh_4 square planes in the static structure.

The Reaction of $[Rh_6(CO)_{13}C]^{2-}$ *with* L–L (*dppm, dppe, dppp, dppb*) *or dpae.*—The reaction of $[NEt_4]_2[Rh_6(CO)_{13}C]$ in solution at room temperature with dppe results in immediate replacement of two carbonyls to give an almost quantitative yield of $[NEt_4]_2[Rh_6(CO)_{11}C(\mu\text{-dppe})]$ (**1**) [equation (2)],

$$2[Rh_6(CO)_{13}C]^{2-} + \text{dppe} \longrightarrow [Rh_6(CO)_{11}C(\mu\text{-dppe})]^{2-} + [Rh_6(CO)_{15}C]^{2-} \quad (2)$$

rather than addition to give the trigonal prismatic cluster, $[Rh_6(CO)_{13}C(dppe)]^{2-}$. Compound (**1**) precipitates as a red-orange powder, which has been recrystallised by stratifying an acetonitrile solution of (**1**) with cyclohexane and then diethyl ether; the mother-liquor was shown to contain $[Rh_6(CO)_{15}C]^{2-}$ from direct ^{103}Rh n.m.r. and i.r. measurements.

Compound (**1**) has been crystallographically characterised (see below) and ^{31}P and direct ^{103}Rh n.m.r. measurements have also been carried out (Table 2). An immediate reaction of $[Rh_6(CO)_{13}C]^{2-}$ with other chelating ligands (dppm, dpae, dppp, dppb) also occurs. Comparison of the spectroscopic data of these products (Table 2) with those of (**1**) suggest that they also adopt a similar structure. Thus, all have three equally intense rhodium resonances in similar positions and, in the case of the chelating diphosphines, exhibit similar rhodium–phosphorus coupling patterns, the central rhodium resonance exhibiting ^1J(Rh–P) and the rhodium resonance at highest frequency usually exhibiting ^2J(Rh–P). This allows this latter resonance to be assigned to the two rhodium atoms [Rh(3) and Rh(6)] which are *trans* to P(2) and P(1) respectively (Figure 4). Furthermore, the weighted mean values of δ(Rh) for all the clusters in Table 2 are similar to those found for (**1**) and not very different to that found for $[Rh_6(CO)_{13}C]^{2-}$ [$\delta(^{103}Rh)_{mean}$ (−96 °C) −744 p.p.m.][10] and $[Rh_6H(CO)_{13}C]^-$ [$\delta(^{103}Rh)_{mean}$ (−90 °C) −675 p.p.m.].

Table 2. Phosphorus-31 and ^{103}Rh n.m.r. data* for $[Rh_6(CO)_{11}C(L\text{–}L)]^{2-}$ (L–L = dppm, dppe, dpae, dppp, dppb) at room temperature

L–L	Solvent	$\delta(^{31}P)$/ p.p.m.	$\delta(^{103}Rh)$/ p.p.m.	$J(^{103}Rh\text{–}^{31}P)$/ Hz	$\delta(^{103}Rh)_{mean}$/ p.p.m.
dppm	EtCN	11.6	−917 (s)	0	−667
			−715 (d)	178	
			−369 (d)	12	
dppe	MeCN	29.7	−921 (s)	0	−709
			−853 (d)	181	
			−362 (d)	11	
dpae	EtCN		−909 (s)		−634
			−636 (s)		
			−358 (s)		
dppp	EtCN	36.1	−914 (s)	0	−664
			−710 (d)	192	
			−369 (d)	10	
dppb	$(CD_3)_2CO$	31.3	−888 (s)	0	−642
			−716 (d)	173	
			−323 (s)	0	

* s = Singlet, d = doublet.

Table 3. Bond lengths (Å)

Rh(2)–Rh(1)	2.736(4)	Rh(4)–Rh(1)	3.064(5)
Rh(5)–Rh(1)	2.965(5)	Rh(6)–Rh(1)	2.839(5)
C–Rh(1)	2.025(17)	P(1)–Rh(1)	2.287(6)
C(1)–Rh(1)	1.898(23)	C(12)–Rh(1)	1.988(18)
Rh(3)–Rh(2)	2.765(5)	Rh(5)–Rh(2)	3.047(5)
Rh(6)–Rh(2)	3.237(5)	C–Rh(2)	2.161(15)
C(12)–Rh(2)	2.077(20)	C(2)–Rh(2)	1.819(20)
C(23)–Rh(2)	2.055(25)		
Rh(4)–Rh(3)	3.183(5)	Rh(5)–Rh(3)	2.925(5)
Rh(6)–Rh(3)	2.780(5)	C–Rh(3)	1.993(16)
C(23)–Rh(3)	2.011(23)	C(3)–Rh(3)	1.856(26)
C(36)–Rh(3)	2.009(23)		
Rh(5)–Rh(4)	2.743(5)	Rh(6)–Rh(4)	2.770(5)
C–Rh(4)	2.137(14)	C(4)–Rh(4)	1.813(18)
C(45)–Rh(4)	2.056(18)	C(46)–Rh(4)	2.014(21)
C–Rh(5)	2.018(17)	P(2)–Rh(5)	2.293(7)
C(45)–Rh(5)	1.999(15)	C(5)–Rh(5)	1.868(19)
C–Rh(6)	2.038(17)	C(1)–Rh(6)	2.682(24)
C(36)–Rh(6)	2.032(19)	C(46)–Rh(6)	2.015(18)
C(6)–Rh(6)	1.816(24)		
C(22)–P(1)	1.843(20)	C(121)–P(1)	1.836(9)
C(221)–P(1)	1.835(12)	C(11)–P(2)	1.834(16)
C(111)–P(2)	1.847(12)	C(211)–P(2)	1.834(11)
C(22)–C(11)	1.590(23)		

X-Ray Structure Characterization of $[NEt_4]_2[Rh_6(CO)_{11}C(\mu\text{-dppe})]$.—In order unambiguously to establish the structure of this series of clusters, we carried out an *X*-ray crystallographic structural determination of $[NEt_4]_2[Rh_6(CO)_{11}C(\mu\text{-dppe})]$ (**1**). The crystal comprises discrete $[Rh_6(CO)_{11}C(\mu\text{-dppe})]^{2-}$ anions (Figure 4) and $[NEt_4]^+$ cations. The metal atom polyhedron is a distorted octahedron containing the interstitial carbide. There are six terminal carbonyls, one per rhodium atom, five bridging carbonyls spanning different edges so that there is an apparent C_2 axis passing through the middle of the Rh(1)–Rh(5) and Rh(3)–Rh(6) edges with dppe spanning the same edge, Rh(1)–Rh(5), as that occupied by H in $[Rh_6H(CO)_{13}C]^-$.

The structure of (**1**) mirrors fairly well that of [Rh$_6$-

$(CO)_{13}C]^{2-}$. The metal–metal distances {with corresponding values found for $[Rh_6(CO)_{13}C]^{2-}$ in parentheses} average 2.92 Å (2.91 Å) and fall into two sets, CO bridged and unbridged, 2.76 Å (2.78 Å) and 3.05 Å (3.04 Å) respectively, with the dppe-bridged edge being 2.965 Å. Similarly, the Rh–$C_{carbide}$ interatomic distances are also related in the two structures with the two longest bonds being to Rh(2) and Rh(4) and the two shortest to Rh(3) and Rh(5) (Table 3).

1,2-Bis(diphenylphosphino)ethane can bridge a variety of metal–metal bond lengths (2.244—3.048 Å)[15–17] and the present value found in (**1**) falls within this range. The preference for phosphine substitution to occur *trans* to formal metal–metal bonds, *viz.* non-bridged metal–metal vectors, is well established for di-, tri-, and tetra-nuclear carbonyls.[18] This appears to be an electronic preference since there is often little stereochemical difference between alternative sites.[19] It is therefore perhaps significant that the structure of (**1**) shows that dppe substitutes in the only equator of the Rh_6 octahedron in $[Rh_6(CO)_{13}C]^{2-}$ which has two non-bridged edges *trans* to each other. This enables dppe to chelate without undue distortion so that phosphorus substitution occurs *trans* to these unoccupied edges, while maintaining the preferred ligand geometry about the Rh_6 octahedron.

It is also worthwhile commenting on other clusters containing bidentate phosphines, which can chelate to give seven- and eight-membered rings, in connection with the other L–L analogues of (**1**). The flexibility of dppb allows different modes of co-ordination but there are presently only two crystallographically characterised examples of clusters containing dppb as a bidentate ligand. In $[Ru_5(CO)_{15}C(\mu\text{-dppb})]$,[20] dppb bridges *opposite* Ru atoms in the square of the Ru_5 square-based pyramid whereas in $[Ru_4(\mu\text{-H})_4(CO)_{10}(\mu\text{-dppb})]$, dppb spans a formal Ru–Ru bond of the Ru_4-tetrahedron to give an eight-membered ring.[21] A related seven-membered ring is found in $[Ru_4(\mu\text{-H})_4(CO)_{10}(\mu\text{-dppp})]$,[21] and there is little variation in the length of the chelated Ru–Ru bond in $[Ru_4(\mu\text{-H})_4(CO)_{10}(\mu\text{-L-L})]$ for L–L = dppm (2.977 Å),[21] dppe (3.0848 Å),[22] dppp (3.061 Å),[21] and dppb (3.004 Å).[21] The related ligand $(Ph_2PCH_2CH_2O)_2CMe_2$, (+)-diop, is also found to form an eight-membered ring by spanning a metal–metal bond in $[Ir_4(CO)_{10}\{(+)\text{-diop}\}]$,[22] which adopts a structure related to $[Rh_4(CO)_{12}]$ with (+)-diop occupying two axial sites on adjacent metals in the basal plane [*d*(Ir–Ir) 2.772 Å]. There is one other *X*-ray structural determination of a compound containing dppp bridging a metal–metal bond, $[Fe_2(CO)_2(\eta^5:\eta^{5'}\text{-}C_5H_4SiMe_2C_5H_4)(\mu\text{-dppp})]$.[23] In this case, although the metal–metal interaction is constrained by the presence of other bridging ligands, there is little difference in *d*(Fe–Fe) on going from dppp (2.521 Å) to dppm (2.497 Å). Thus it appears that various bridging L–L ligands can bridge similar metal–metal bonds by adopting different conformations. This, coupled with the spectroscopic data described earlier, is entirely consistent with $[Rh_6(CO)_{11}C(\mu\text{-L-L})]^{2-}$ (L–L = dppm, dppe, dppp, dppb, dpae) all adopting similar structures to (**1**).

Table 4. Atomic co-ordinates (× 10^4)

Atom	*x*	*y*	*z*
Rh(1)	6 263(1)	8 011(1)	2 000(1)
Rh(2)	4 302(1)	6 220(1)	2 247(1)
Rh(3)	3 641(1)	7 313(1)	3 185(1)
Rh(4)	6 065(1)	9 378(1)	3 125(1)
Rh(5)	6 158(1)	7 321(1)	3 338(1)
Rh(6)	4 226(1)	8 684(1)	2 156(1)
C	5 105(13)	7 819(11)	2 688(7)
P(1)	8 275(3)	8 371(3)	1 835(2)
P(2)	7 885(4)	6 845(3)	3 398(2)
C(11)	9 201(13)	7 728(11)	3 003(7)
C(22)	9 113(15)	7 563(11)	2 258(7)
C(111)	8 580(11)	6 820(9)	4 208(4)
C(112)	9 609(11)	7 677(9)	4 444(4)
C(113)	10 121(11)	7 633(9)	5 056(4)
C(114)	9 603(11)	6 734(9)	5 433(4)
C(115)	8 574(11)	5 878(9)	5 197(4)
C(116)	8 062(11)	5 921(9)	4 585(4)
C(211)	7 779(9)	5 484(6)	3 119(5)
C(212)	8 785(9)	5 131(6)	3 186(5)
C(213)	8 669(9)	4 079(6)	2 988(5)
C(214)	7 547(9)	3 380(6)	2 724(5)
C(215)	6 540(9)	3 733(6)	2 657(5)
C(216)	6 656(9)	4 785(6)	2 855(5)
C(121)	9 313(8)	9 780(6)	1 980(5)
C(122)	8 860(8)	10 563(6)	2 198(5)
C(123)	9 625(8)	11 648(6)	2 278(5)
C(124)	10 843(8)	11 950(6)	2 140(5)
C(125)	11 296(8)	11 167(6)	1 922(5)
C(126)	10 531(8)	10 082(6)	1 842(5)
C(221)	8 533(10)	8 166(9)	1 012(4)
C(222)	8 740(10)	7 227(9)	818(4)
C(223)	8 871(10)	7 072(9)	182(4)
C(224)	8 795(10)	7 856(9)	−259(4)
C(225)	8 589(10)	8 795(9)	−65(4)
C(226)	8 458(10)	8 950(9)	571(4)
C(1)	5 846(16)	8 803(16)	1 311(10)
O(1)	5 797(14)	9 196(15)	832(7)
C(12)	5 766(15)	6 470(13)	1 698(8)
O(12)	6 082(12)	5 933(10)	1 360(7)
C(2)	3 604(18)	4 895(15)	1 854(9)
O(2)	3 170(16)	4 053(12)	1 614(9)
C(23)	2 817(17)	5 833(16)	2 776(13)
O(23)	1 917(15)	5 110(14)	2 839(11)
C(3)	2 724(20)	7 045(18)	3 833(11)
O(3)	2 209(19)	6 875(15)	4 321(9)
C(36)	2 822(15)	8 270(16)	2 725(8)
O(36)	1 982(12)	8 571(13)	2 805(7)
C(4)	6 888(18)	10 668(14)	3 528(8)
O(4)	7 453(18)	11 477(11)	3 791(8)
C(45)	7 077(14)	8 759(11)	3 762(7)
O(45)	7 828(12)	9 088(9)	4 183(6)
C(46)	5 193(16)	10 160(14)	2 543(8)
O(46)	5 168(14)	11 051(10)	2 433(7)
C(5)	5 332(17)	6 380(13)	3 953(9)
O(5)	4 986(14)	5 752(11)	4 332(7)
C(6)	3 395(18)	9 117(18)	1 506(10)
O(6)	2 894(18)	9 403(17)	1 079(9)
N(1a)	3 348(15)	1 659(14)	4 051(8)
C(11a)	2 111(16)	1 425(18)	4 238(10)
C(12a)	1 092(20)	678(19)	3 776(11)
C(21a)	3 609(29)	649(19)	3 971(14)
C(22a)	3 487(27)	−78(24)	4 560(13)
C(31a)	4 164(19)	2 382(20)	4 545(11)
C(32a)	5 538(20)	2 758(21)	4 423(12)
C(41a)	3 530(27)	2 158(22)	3 430(10)
C(42a)	3 278(28)	3 248(22)	3 422(15)
N(1b)	6 709(26)	3 047(23)	472(14)
C(11b)	5 544(32)	2 179(34)	504(23)
C(12b)	4 815(39)	2 468(35)	1 004(20)
C(21b)	6 710(48)	2 710(43)	−176(16)
C(22b)	7 825(48)	3 413(46)	−513(28)
C(31b)	6 720(42)	4 160(25)	410(22)
C(32b)	6 334(70)	3 802(65)	−285(24)
C(41b)	7 493(38)	2 677(36)	905(18)
C(42b)	7 782(50)	1 761(40)	566(25)

Experimental

General.—^1H-{^{103}Rh} INDOR, ^{13}C, ^{13}C-{^{103}Rh}, and ^{103}Rh n.m.r. measurements were carried out as described previously.[7,24–26] Internal $SiMe_4$ was used as a reference for ^1H and ^{13}C chemical shifts. Values of $\delta(^{103}Rh)$ are derived from a standard frequency, 0 p.p.m. = 3.16 MHz, at such a magnetic field that the protons in $SiMe_4$ resonate at exactly 100 MHz. All operations were carried out under a nitrogen atmosphere and solvents were distilled and dried using the usual methods.

Preparation of $[Rh_6H(CO)_{13}C]^-$.—To a solution of $[PPh_3(CH_2Ph)]_2[Rh_6(CO)_{13}C]$[1] (0.3 g) in CH_2Cl_2 (3 cm^3) in an n.m.r. tube at -78 °C was added CF_3CO_2H (*ca.* 0.1 cm^3; this is an excess of acid, *viz.* $Rh_6:H^+ =$ *ca.* 1:7.4). There was an immediate reaction and the multinuclear n.m.r. characterisation was carried out directly on this solution without allowing it to warm > -20 °C.

On allowing the solution to warm > -20 °C, CO was evolved and the i.r. spectrum of the resulting solution corresponded exactly with that previously reported for $[Rh_{12}(CO)_{24}(C)_2]^{2-}$.[13]

Preparation of $[NEt_4]_2[Rh_6(CO)_{11}C(\mu\text{-dppe})]$ (**1**).—To a solution of $[NEt_4]_2[Rh_6(CO)_{13}C]$ (1.2 g, 0.96 mmol) in tetrahydrofuran (thf) (20 cm^3) was added a solution of dppe (0.19 g, 0.48 mmol) in thf (6 cm^3). There was an immediate precipitation of a red solid which was filtered off and dried. The filtrate was shown by both ^{103}Rh n.m.r. and i.r. measurements to contain $[NEt_4]_2[Rh_6(CO)_{15}C]$. Crystals of (**1**), suitable for *X*-ray analysis, were produced by dissolution of the red precipitate in acetonitrile followed by stratification with cyclohexane and then diethyl ether. The yield based on equation (2) was 80—90%. The i.r. spectrum of (**1**) in MeCN in the carbonyl stretching region showed bands at 1 951s and 1 790m cm^{-1}.

Similar i.r. spectra were obtained for the analogous derivatives of (**1**) which were prepared in a similar way by addition of the appropriate ligand [ν(CO)/cm^{-1}: L–L = dppm, 1 949s, 1 800m; dppp, 1 965s, 1 825m; dppb, 1 963s, 1 808m].

Crystallography.—*Crystal data.* $C_{56}H_{40}N_2O_{13}P_2Rh_6$, $M = 1\,638.33$, triclinic, space group $P1$, $a = 11.677(2)$, $b = 13.001(2)$, $c = 21.230(3)$ Å, $\alpha = 89.22(1)$, $\beta = 94.59(1)$, $\gamma = 109.77(1)°$, $U = 3\,020$ Å^3, $Z = 2$, $D_c = 1.79$ g cm^{-3}, $\lambda = 0.710\,69$ Å, $\mu(\text{Mo-}K_\alpha) = 19.65$ cm^{-1}.

The structure was solved *via* direct methods and developed and refined *via* Fourier and full-matrix least-squares procedures using 6 782 observed [$I > 1.50\sigma(I)$] data from a total of 10 588 measured on a CAD4 diffractometer. The data were corrected for absorption on the basis of azimuthal scan measurements. The final R value was 0.064, with only atoms in the cluster anion assigned anisotropic thermal parameters. The phenyl rings in the anion were treated as idealised rigid bodies with C–C 1.395 Å, C–C–C 120°.

The atomic co-ordinates for the anion are reported in Table 4, and the bond distances in Table 3. Additional material available from the Cambridge Crystallographic Data comprises thermal parameters and remaining bond lengths and angles.

Acknowledgements

We thank the S.E.R.C. for financial support (to S. B., C. S., and L. S.), for high-field n.m.r. services (Dr. I. H. Sadler, Edinburgh), and for provision of a diffractometer at Q.M.C. and the National Research Council of Italy (C.N.R.) for financial support.

References

1 V. G. Albano, D. Braga, and S. Martinengo, *J. Chem. Soc., Dalton Trans.*, 1981, 717.

2 V. G. Albano, D. Braga, and S. Martinengo, *J. Chem. Soc., Dalton Trans.*, 1986, 981.

3 G. Ciani and S. Martinengo, *J. Organomet. Chem.*, 1986, **306**, C49.

4 S. Martinengo, G. Ciani, A. Sironi, B. T. Heaton, and J. Mason, *J. Am. Chem. Soc.*, 1980, **101**, 7095.

5 R. Bonfichi, G. Ciani, A. Sironi, and S. Martinengo, *J. Chem. Soc., Dalton Trans.*, 1983, 253.

6 V. G. Albano, M. Sansoni, P. Chini, and S. Martinengo, *J. Chem. Soc., Dalton Trans.*, 1973, 651.

7 B. T. Heaton, L. Strona, S. Martinengo, D. Strumolo, R. J. Goodfellow, and I. H. Sadler, *J. Chem. Soc., Dalton Trans.*, 1982, 1499.

8 V. G. Albano, P. L. Bellon, and M. Sansoni, *J. Chem. Soc. A*, 1971, 678.

9 G. Ciani, A. Sironi, P. Chini, and S. Martinengo, *J. Organomet. Chem.*, 1981, **213**, C37.

10 B. T. Heaton, L. Strona, and S. Martinengo, *J. Organomet. Chem.*, 1981, **215**, 415.

11 D. Braga and B. T. Heaton, *J. Chem. Soc., Chem. Commun.*, 1987, 608.

12 C. Allevi, B. T. Heaton, C. Seregni, L. Strona, R. J. Goodfellow, P. Chini, and S. Martinengo, *J. Chem. Soc., Dalton Trans.*, 1986, 1375.

13 V. G. Albano, D. Braga, P. Chini, D. Strumolo, and S. Martinengo, *J. Chem. Soc., Dalton Trans.*, 1983, 249.

14 V. G. Albano, D. Braga, D. Strumolo, C. Seregni, and S. Martinengo, *J. Chem. Soc., Dalton Trans.*, 1985, 1309.

15 F. A. Cotton, G. G. Stanley, and R. A. Walton, *Inorg. Chem.*, 1978, **17**, 2099.

16 F. A. Cotton, T. R. Felthouse, and R. G. Lay, *J. Am. Chem. Soc.*, 1980, **102**, 1431.

17 M. R. Churchill, R. A. Lashewycz, J. R. Shapley, and S. I. Richter, *Inorg. Chem.*, 1980, **19**, 1277.

18 B. T. Heaton, *A.C.S. Symp. Ser.*, 1983, 227.

19 A. S. May, Ph.D. Thesis, University of Western Australia, 1986.

20 J. Evans, B. P. Gracey, L. R. Gray, and M. Webster, *J. Organomet. Chem.*, 1982, **240**, C61.

21 J. Puga, A. Arce, D. Braga, N. Centritto, F. Grepioni, R. Castillo, and J. Ascanio, *Inorg. Chem.*, 1987, **26**, 867.

22 D. Tranqui, A. Durif, M. N. Eddine, J. Lieto, J. J. Raffalko, and B. C. Gates, *Acta Crystallogr., Sect. B*, 1982, **38**, 1916.

23 M. E. Wright, T. M. Mezza, G. D. Nelson, N. R. Armstrong, V. W. Day, and M. R. Thompson, *Organometallics*, 1983, **2**, 1711.

24 P. L. Goggin, R. J. Goodfellow, J. R. Knight, M. G. Norton, and B. F. Taylor, *J. Chem. Soc., Dalton Trans.*, 1973, 2220.

25 G. Longoni, B. T. Heaton, and P. Chini, *J. Chem. Soc., Dalton Trans.*, 1980, 1537.

26 C. Brown, B. T. Heaton, L. Longhetti, W. T. Povey, and D. O. Smith, *J. Organomet. Chem.*, 1980, **192**, 93.

Received 23*rd September* 1987; *Paper* 7/1706